UCSF

Title

White matter injury in term neonates with congenital heart diseases: Topology & comparison with preterm newborns

Permalink

Authors

Guo, Ting

Chau, Vann

Peyvandi, Shabnam

et al.

Publication Date

DOI

Peer reviewed

White Matter Injury in Term Neonates with Congenital Heart Diseases: Topology & Comparison with Preterm Newborns

Ting Guo, PhD[1,2], **Vann Chau, MD**[1,2], **Shabnam Peyvandi, MD**[8], **Beatrice Latal, MD**[10], **Patrick S. McQuillen, MD**[7], **Walter Knirsch, MD**[11], **Anne Synnes, MDCM**[3], **Maria Feldmann**[10], **Nadja Naef**[10], **M. Mallar Chakravarty, PhD**[4,5,6], **Alessandra De Petrillo, MSc**[1], **Emma G. Duerden, PhD**[1,2], **A. James Barkovich, MD**[9], and **Steven P. Miller, MDCM**[1,2]

[1] Neurosciences and Mental Health, The Hospital for Sick Children Research Institute, Toronto, ON, Canada [2] Department of Paediatrics, The Hospital for Sick Children and the University of Toronto, Toronto, ON, Canada [3] Department of Pediatrics, University of British Columbia, and BC Children's Hospital Research Institute, Vancouver, BC, Canada [4] Cerebral Imaging Centre, Douglas Mental Health Research Institute, Verdun, QC, Canada [5] Department of Psychiatry, McGill University, Montreal, QC, Canada [6] Biological and Biomedical Engineering, McGill University, Montreal, QC, Canada [7] Department of Pediatrics, Benioff Children's Hospital and University of California, San Francisco, CA, USA [8] Department of Pediatric Cardiology, Benioff Children's Hospital and University of California, San Francisco, CA, USA [9] Department of Radiology, Benioff Children's Hospital and University of California, San Francisco, CA, USA [10] Child Development Center, University Children's Hospital, Zurich, Switzerland [11] Department of Pediatric Cardiology, University Children's Hospital, Zurich, Switzerland

Abstract

Background: Neonates with congenital heart disease (CHD) are at high risk of punctate white matter injury (WMI) and impaired brain development. We hypothesized that WMI in CHD neonates occurs in a characteristic distribution that shares topology with preterm WMI and that lower birth gestational age (GA) is associated with larger WMI volume.

Objective: (1) To quantitatively assess the volume and location of WMI in CHD neonates across three centres. (2) To compare the volume and spatial distribution of WMI between term CHD neonates and preterm neonates using lesion mapping.

Methods: In 216 term born CHD neonates from three prospective cohorts (mean birth GA: 39 weeks), WMI was identified in 86 neonates (UBC: 29; UCSF: 43; UCZ: 14) on pre- and/or post-operative T1 weighted MRI. WMI was manually segmented and volumes were calculated. A standard brain template was generated. Probabilistic WMI maps (total, pre- and post-operative) were developed in this common space. Using these maps, WMI in the term CHD neonates was

Corresponding author: Steven P. Miller, Hospital for Sick Children, 555 University Avenue, Toronto, Ontario, Canada M5G 1X8, Phone: 1-416-813-6659, Fax:1-416-813-6334, steven.miller@sickkids.ca.

compared with that in preterm neonates: 58 at early-in-life (mean postmenstrual age at scan 32.2 weeks); 41 at term-equivalent age (mean postmenstrual age at scan 40.1 weeks).

Results: The total WMI volumes of CHD neonates across centres did not differ (p=0.068): UBC (median=84.6mm^3, IQR=26–174.7mm^3); UCSF (median=104mm^3, IQR=44–243mm^3); UCZ (median=121 mm^3, IQR=68–200.8mm^3). The spatial distribution of WMI in CHD neonates showed strong concordance across centres with predilection for anterior and posterior rather than central lesions. Predominance of anterior lesions was apparent on the post-operative WMI map relative to the pre-operative map. Lower GA at birth predicted an increasing volume of WMI across the full cohort (41.1mm^3 increase of WMI per week decrease in gestational age; 95% CI 11.5–70.8; p=0.007), when accounting for centre and heart lesion. While WMI in term CHD and preterm neonates occurs most commonly in the intermediate zone/outer subventricular zone there is a paucity of central lesions in the CHD neonates relative to preterms.

Conclusions: WMI in term neonates with CHD occurs in a characteristic topology. The spatial distribution of WMI in term neonates with CHD reflects the expected maturation of pre-oligodendrocytes such that the central regions are less vulnerable than in the preterm neonates.

1. INTRODUCTION

Congenital heart disease (CHD) is now the most common birth defect impacting almost 1% of live births (Marelli2016). Although the survival of neonates with critical CHD has been dramatically improved over the past three decades, the neurodevelopmental morbidity of this population remains high (Marelli2016). Advances in neuroimaging have enabled the detection of brain injury and delayed brain development and maturation reflected in reduced brain volumes and altered brain microstructure and metabolism in the term CHD population (Andropoulos2010, Clouchoux2013, Dimitropoulos2013, *Karmacharya2018,* Licht2009, Miller2007, Partridge2006, von Rhein2015). The impaired oxygen and nutrient delivery secondary to the disordered fetal and post-natal circulation associated with the congenital heart lesion contributes to brain injury and impaired brain development in newborns with CHD (Lim2016, Limperopoulos2010, Rudolph2016, Sun2015). Yet, the mechanism of neurodevelopmental disability in children with CHD is likely multifactorial, with a cumulative and complex interplay of cardiovascular physiology and brain abnormalities (Marelli2016, Morton2017).

Brain injuries, particularly white matter injury (WMI) and small strokes are now routinely reported in neonates with CHD (Beca2013, Dimitropoulos2013, McQuillen2007). WMI is the most consistently identified pattern of brain injury in the term neonates with CHD (Licht2004, Mahle2002, McQuillen2007, Miller2004). Previous studies have demonstrated that lower birth GA in term neonates with CHD is associated with higher mortality and worse neurodevelopmental outcomes (Goff2012, Steurer2017). Yet, the link between the extent of WMI in the term neonate with CHD and birth GA is uncertain.

WMI in term neonates with CHD seems to resemble that identified commonly in preterm neonates (Beca2013, Dimitropoulos2013, Guo2017, McQuillen & Miller2010, Peyvandi2016). In preterm neonates, WMI is readily visualized on T1-weighted MRI acquired in the first weeks of life as areas of hyper-intensity, with a predilection for the central periventricular white matter (Guo2017, Miller & Back2014, Raybaud2013). WMI in preterm neonates is related to the selective vulnerability and maturation arrest of the pre-oligodendrocyte (pre-OL), with the topography of WMI predicted by the spatial distribution of these vulnerable cells (Riddle2006). However, the spatial distribution of WMI in these two populations has never been rigorously compared. As the relationship of WMI with 18-month neurodevelopmental outcomes in preterm neonates is mediated by lesion volume as well as by lesion location, understanding the spatial distribution of WMI in the term neonate with CHD is an important next step (Guo2017).

To fully characterize WMI in term neonates with CHD, we quantitatively assessed the volume and location of WMI and developed probabilistic WMI maps. We examined clinical risk factors for WMI *volumes,* hypothesizing that younger gestational age at birth would predict greater WMI volume, independent of other established clinical risk factors for WMI. Oligodendrocyte progenitor cells in supratentorial white matter demonstrate regional variability in their maturation: earlier maturation in central regions, followed by posterior and then anterior white matter (Volpe2000). Therefore, we compared the pre- and post-operative WMI in CHD neonates and hypothesized that these neonates would exhibit a posterior to anterior predominance of WMI that coincides with the expected progression of oligodendrocyte lineage maturation. We then compared the probabilistic maps in neonates with CHD relative to maps developed in preterm neonates scanned with similar parameters. We hypothesized that WMI in term neonates with CHD would be most prevalent in anterior and posterior, rather than central white matter.

2. METHODS

2.1 Study Population

225 term born neonates with congenital heart diseases (CHD) (149 boys, 66.2%, mean birth GA: 39 weeks) who were admitted to British Columbia's Women's Hospital, University of British Columbia (UBC), the University of California San Francisco Benioff Children's Hospital (UCSF), or University Children's Hospital Zurich (UCZ) were enrolled in prospective cohort studies at each centre. Of these newborns, nine were excluded for congenital infections or genetic disorders, or because surgery was delayed beyond 3 months of life, for a final cohort of 216 neonates. Clinical data of these CHD neonates were collected prospectively and are summarized in Table 1. Cardiac diagnoses included patients with D-Transposition of the great arteries (n=118), single ventricle physiology (n=64), and others lesions (n=29) such as double outlet right ventricle (DORV), ventricular septal defect (VSD), and tetralogy of Fallot (TOF).

Written informed consents were obtained from the legal guardians of enrolled neonates. The Clinical Research Ethics Board at each study site reviewed and approved the study.

2.2 Brain Imaging and Injury Scoring

A total of 186 (UBC: 69, UCSF: 106, UCZ: 11) pre-operative (median age: 39.7 weeks; IQR=38.7–40.8) and 172 (UBC: 58, UCSF: 101, UCZ: 13) post-operative (median age: 42.1 weeks; IQR=40.7–43.4) scans were acquired during the study period *using optimized scanning protocols with dedicated neonatal head coils at UBC and UCSF.* 161 neonates had both pre- and post-operative scans. Brain MRI acquisition were carried out on a 1.5T Siemens Avanto scanner (Erlangen, Germany) at UBC, on a 1.5T GE Signa Echo-Speed system and a 3T GE Signa Discovery MR750 system (Waukesha, USA) at UCSF, and on a 3T GE Signa HDxt (Waukesha, USA) at UCZ. The following MRI parameters were used for the 3D volumetric T1-weighted acquisitions (TR/TE/FOV/slice thickness/Gap/flip angle): UBC: 36ms/9.2ms/20cm/1mm/0mm/30°/; UCSF: 1.5T 35ms/6ms/22cm/1mm/0mm/35°, 3T 10.4ms/4.3ms/18–20cm/1mm/0mm/15°/TI: 450ms; UCZ: 11.4ms/4.8ms/18–20cm/1mm/0mm/13°/TI: 450ms.

Brain abnormalities on each MRI were scored by experienced neuroradiologists blinded to the clinical history of each neonate (Dimitropoulos2013) with demonstrated high inter-rater reliability of the scores used to assess on the severity of brain injury (Block2010).

2.3 Quantitative Assessment of WMI

Punctate WMI was characterized as areas of T1 hyperintensity and was manually delineated on 109 scans: 50 pre-operative [median age: 40 weeks, IQR: 38.6–41.2] and 59 post-operative [median age: 41.9 weeks, IQR: 40.5–43.2]) 3D T1-weighted images of 86 term CHD neonates by a trained rater (TG) and reviewed by an experienced neonatal neurologist (SPM). *Display software (http://www.bic.mni.mcgill.ca/ServicesSoftwareVisualization) that allows simultaneous view of the brain on coronal, axial, and sagittal planes was used for manual WMI segmentation. Tricubic interpolation permitted consistent differentiation of WMI from surrounding tissue and only those voxels containing over 50% of WMI were considered. High inter-rater reliability was achieved in WMI segmentation with an average Dice's Kappa value of 0.81. The total WMI volume and the percentage of WMI volume to total brain volume of each neonate were calculated based on the manual segmentation of all punctate WMI lesions on the brain image (number of lesions 1).* Detailed methods were previously described (Guo2017). If WMI was identified on both the pre- and postoperative T1-weighted images of a neonate, the largest total WMI volume was included in the statistical analysis.

2.4 White Matter Injury Maps for Term Neonates with CHD

To assess the WMI pattern in the brain of the term CHD population, probabilistic WMI maps were developed: (1) the total probabilistic WMI map, and (2) the pre- and post-operative WMI maps. A brain template of term CHD neonates was specifically built as the common space for the development of the WMI maps. MICe-build-model (Friedel2014) was used to create the template with 64 quality-inspected and age-appropriate T1-weighted images (median age: 40.3 weeks, IQR=39.7–40.7).

The total WMI map was generated by nonlinearly mapping (Avants2008) the manually segmented WMI from each neonate brain image to the CHD brain template, incorporating

the WMI of all 86 neonates. The colour of each voxel on the map reflects the cumulative number of patients who had WMI lesions at the homologous brain region. This map depicts the spatial distribution pattern of WMI across patients within the common brain space and demonstrates the brain regions that are vulnerable to WMI in term CHD neonates. Using the same method, a separate WMI map was also created for the neonates from each centre (UBC: 29 neonates, UCSF: 43 neonates, UCZ: 14 neonates).

Since the maturation of the oligodendrocyte progenitor cells in supratentorial white matter follows a central to posterior to anterior trajectory (Volpe2000), we developed two separate WMI maps representing the pre- and post-operative WMI respectively to assess if any distinguished spatial distribution pattern exits between the pre- and post-operatively identified WMI. The WMI lesion areas that are common to both pre- and post-operative images and unique to each group are represented in different colours (Common: white; pre-operative only: magenta; post-operative only: blue).

A high-performance nonlinear registration algorithm (Avants2008) was used to ensure accurate mapping of WMI from each neonate to the brain template. Registration results were assessed by visually examining the overlap of homologous regions of the CHD brain template and the brain image of each neonate registered to the template. Furthermore, to account for potential anatomical variability, punctate WMI that occurred in two or more term CHD neonates at a homologous region on each WMI map were considered and WMI lesions seen only in a single neonate were omitted.

2.5 Comparison of WMI between Term CHD and Very Preterm Neonates

As WMI is the characteristic brain injury pattern in preterm neonates (Miller & Back2014, Guo2017), we compared the total WMI volumes of the 86 CHD neonates (median birth GA: 39.6 weeks, IQR: 38.6–40.9) with those of the 58 preterm neonates (median birth GA: 28.6 weeks, IQR: 26.3–29.8), adjusting for birth GA, sex, age at scan, and total brain volume. *The 58 preterm neonates were from a single centre study and their T1-weighted images were acquired on the same scanner as those of the 29 CHD neonates from UBC using similar imaging protocols.* The detailed information of these 58 preterm neonates was described previously (Guo2017). The probabilistic WMI maps of the preterm neonates at early-in-life and term-equivalent age (TEA) were nonlinearly transformed from the preterm brain to the term CHD brain space to allow direct voxel-wise comparison of WMI distribution in these two high-risk populations. Three distinguished colours were used to represent the lesions that were either common and unique to preterm and CHD neonates to better visualize the cross-population comparison.

2.6 Data Analyses

Statistical analyses were carried out using the Statistical Package for the Social Sciences (SPSS, v24, IBM). Clinical and demographic variables between the three centres were compared using Kruskal-Wallis tests (continuous data) and Chi-square or Fisher's exact tests (categorical data). P values <0.05 were considered statistically significant.

The association between total WMI *volume* and gestational age at birth was examined using multivariable linear regression to account for heart lesion and centre. We then examined

whether this relationship was independent of established clinical risk factors for WMI: lowest pre-operative arterial saturation, total cardiopulmonary bypass time, and lowest mean blood pressure post-operatively.

3. RESULTS

3.1 Study Participants and Clinical Evaluation

Despite differences in several clinical variables across centres, *the timing of MRI and the incidence of stroke did not differ* (see Table 1 for cross centre comparisons).

86 of 216 term newborns with CHD from three centres had WMI on their pre- and/or post-operative MRI: 26.9% pre-operatively and 34.3% post-operatively (new lesions 20.9%). *Ranging from minimum of 7 mm^3 to maximum of 3212 mm^3 (median 88 mm^3), the total WMI volumes of neonates from the three centres were comparable (p=0.068) (Figure 1).* The total WMI volume (219.4 ± 490.0 mm^3) identified on the 50 pre-operative images was similar to the total WMI volume (199.2 ± 346.4 mm^3) on the 59 post-operative images.

We then examined the clinical factors associated with WMI volumes in this cohort of term neonates with CHD. An increasing volume of WMI across the full cohort (three centres) was predicted by lower gestational age at birth (41.1mm^3 increase per week decrease gestational age; 95% CI 11.5–70.8; p=0.007), when accounting for centre and heart lesion. To account for differences in brain size across gestational ages, we also examined the volume of WMI as a percentage of total brain volume with similar findings (0.015% increase WMI per week decrease gestational age; 95% CI 0.0055%–0.025%; p=0.002), accounting for centre and heart lesion.

We then examined whether this relationship was confounded by established clinical predictors of WMI in term neonates with CHD, such as lowest arterial saturation, total cardiopulmonary bypass time, and lowest mean blood pressure. Even when accounting for these other clinical factors, lower gestational age at birth remains a robust predictor of total WMI volume, and WMI volume as a percent of total brain volume (Table 2a). The relationship of lower gestational age at birth predicting higher maximum WMI volumes remains significant, even when accounting for the day of life at surgery in this multivariable model (24.6mm^3 increase in WMI per week decrease in birth GA, P=0.013, 95% CI 5.4 –43.7). Finally, we restricted our analysis to the volume of WMI pre-operatively, and find that lower gestational age at birth is even more robustly associated with larger WMI volumes, even when accounting for potential confounding variables (Table 2b).

3.2 WMI Distribution Pattern in the 3D Brain Space of Term CHD Neonates

The probabilistic WMI map of the 86 CHD neonates with WMI demonstrated that the occurrence of WMI follows a characteristic spatial pattern with predilection for anterior and posterior rather than central lesions (Figure 2a). *Accurate registration of all images to the brain template was achieved and excellent overlap was found in homologous regions of the template and the brain image registered to the template. The registration accuracy is particularly optimized in the subcortical regions, where WMI is located.* Strong concordance in WMI spatial distribution was observed across the three centres (Figure 2b). WMI in term

neonates with CHD were mainly distributed in the intermediate zone (IZ) and/or subventricular zone (SVZ) (Figure 2c). The post-operatively identified WMI had predominance in the anterior regions relative to the pre-operative WMI (Figure 3).

3.3 WMI in Term CHD Neonates relative to Preterm Neonates

The total WMI volumes in 86 CHD neonates and 58 preterm neonates was not significantly different, controlling for birth GA, sex, and age at scan, and total brain volume. As shown on Figure 1, WMI evolves from birth to term with the volume of WMI at TEA in the majority of preterm neonates being smaller than that at early-in-life. When the WMI of 86 term CHD neonates was compared with that of preterm neonates (58 at early-in-life and 41 at TEA) in the same brain template (Figure 4), it was apparent that WMI of CHD neonates extended more anteriorly and posteriorly with a paucity of central lesions relative to that of preterm neonates.

4. DISCUSSION

In this multi-centre study, we demonstrate that WMI in term neonates with CHD has a characteristic volume and distribution pattern in the brain. Importantly, there was strong concordance in the spatial distribution and burden of WMI across the three centres. The topology of pre- and post-operatively identified WMI coincides with the expected regional maturation of the oligodendrocyte lineage and supports the selective vulnerability of the oligodendrocyte progenitor cells in the pathophysiology of WMI (Volpe2000). A voxel-wise comparison of WMI between preterm neonates and those with CHD was enabled by nonlinearly accommodating anatomical variability. In support of this idea, term neonates with CHD have WMI with a predilection for posterior and anterior white matter in contrast with the central predominance of WMI in the neonate born preterm.

Over the last two decades, WMI has emerged as the most prevalent pattern of brain injury in the term neonate with CHD (Beca2013, McQuillen2007, Petit2009). WMI is the expected pattern of brain injury in the preterm neonate given that the white matter in the third trimester of gestation has an abundance of pre-oligodendrocytes (pre-OLs). Pre-OLs are recognized to be exquisitely sensitive to hypoxia-ischemia, inflammation, and energy deprivation (Back2014; Buser2012). By term-equivalent age, the white matter pre-OLs have largely matured to immature oligodendrocytes, a more resistant cell type, explaining the much less frequent occurrence of WMI in term neonates exposed to hypoxia ischemia (Li2009). Thus, the unexpected frequency of WMI in term neonates with CHD suggested a delay in brain maturation (i.e. dysmaturation) such that these term neonates respond to a brain insult with a pattern of brain injury expected in preterms.

Brain dysmaturation in term neonates with CHD is now recognized pre-operatively as reflected in abnormal brain maturation (Licht2009), volume (von Rhein2015), microstructure and metabolism (Miller2007). The onset of this brain dysmaturation begins in the third trimester of gestation as demonstrated by fetal MRI and MRS (Limperopoulos2010). Thus, we infer that brain dysmaturation provides the substrate for WMI in the term neonate with CHD. Given the later occurrence of WMI in the term neonates with CHD, relative to the preterm neonates in whom the frequency of WMI peaks

at 28 weeks gestation, we hypothesized that we would see a paucity of central WMI as the pre-OLs in this area mature before those in posterior and anterior brain regions. Our findings support this hypothesis and the link between delayed brain maturation and WMI in the neonate with CHD.

As demonstrated previously, WMI in preterm neonates has its prevalence in the intermediate zone (IZ) and/or subventricular zone (SVZ) (Kostovic2002, Guo2017). *Although clear differentiation of IZ and SVZ remains challenging without specific histological markers (Fietz2010, Martinez-Cerdeno2012), based on the cross-population comparison, the WMI in CHD neonates appears to be similarly distributed to preterms in regards to the "white matter layers" (Figure 4). Multiple neuroimaging studies have found association of WMI with impaired white matter maturation, microstructure, and connectivity in both preterm neonates (Adams2010, Bassi2011, He2015, Smyser2013, Tusor2017) and term neonates with CHD (Andropoulos2010, Dimitropoulos2013, Mulkey2014, Partridge2006, von Rhein2015). WM microstructure in the corticospinal tract was particularly affected by WMI in preterm neonates at TEA (Bassi2011) and newborns with CHD (Mulkey2014, Partridge2006) as reflected in reduced fractional anisotropy (FA) values. Our findings suggest that the Corona radiata/centrum semiovale and posterior periventricular WM are the most vulnerable to WMI in CHD newborns. WMI is emerging as a strong predictor of adverse neurodevelopmental outcome at 30 months in term CHD neonates (Peyvandi2018) and increased WMI volume was associated with worse motor outcomes at 18 months in preterm neonates (Guo2017). As WMI occurs at regions that overlap with important projection and association fibres, such as the cortico-spinal tract and superior longitudinal fasciculus (SLF), it is not surprising that WMI poses greater risk to neurodevelopmental functions that are primarily subserved by these regions. This hypothesis is supported by the quantitative WMI assessment in preterm neonates which revealed that WMI lesion locations rather than volumes on early scans have greater predictive value to adverse cognitive and motor outcomes (Guo2017).* It is also important to recognize the complex interplay of delayed brain development and injury in this population, such that the injuries themselves are associated with further impairments in subsequent brain maturation (Andropoulous2010, Dimitropoulos2013, Patridge2006).

Interestingly, the maximal volume of WMI was robustly predicted by lower gestational age at birth, even when accounting for heart lesion and previously established clinical risk factors for WMI. Lower gestational age at birth superseded these other clinical risk factors in magnitude for predicting the extent of WMI. This relationship persisted when accounting for age at surgery. As expected, the relationship between lower gestational age and increasing WMI volume was particularly apparent when examining of pre-operative WMI. The importance of lower gestational age as a predictor of WMI is consistent with the hypothesis that brain dysmaturation is the key substrate for the occurrence of this "preterm pattern" of brain injury in the *term* newborn with CHD (Miller & Back 2014). This finding is also consistent with observations that lower gestational age at birth in the term neonate with CHD predicts higher mortality (Steurer2017) and worse neurodevelopmental outcomes (Goff2012). These findings complement descriptions of impaired in utero brain maturation related to reductions in cerebral oxygen delivery from CHD (Sun2015). Our findings suggest two main sources contributing brain dysmaturation in term neonates with CHD: the *in utero*

effects of CHD and slightly earlier delivery. Determining how these two competing factors interact requires further study in cohorts with fetal imaging.

We included the maximum WMI volume of each *CHD* neonate in our analyses when WMI was identified on multiple images of the same participant. *The age at MRI for these neonates across the three centres was comparable.* The quantitative comparison between CHD and preterm neonates on WMI load was made with the WMI volumes measured early-in-life for the preterm population to allow more accurate representation of the burden of WMI at its peak vulnerability (Martinez-Biarge2016). The quantification of WMI is limited by the spatial resolution of the brain MRI yet our findings reflect clinically accessible imaging resolution. Long-term follow-up of these cohorts is warranted to comprehensively assess functional outcomes that are tightly linked to anterior (e.g. executive function, motor planning) and posterior brain regions (e.g. vision, facial recognition). Longer term follow-up of cohorts with neonatal imaging are also needed to determine how early brain injuries contribute to the relationship of brain volumes and functional outcomes reported in adolescence (von Rhein2014). *Although in our initial analysis, we did not find any significant association between the presence of the WMI and the total cerebral volume (TCV) (p=0.35),* the relationship between WMI and regional gray matter volume deserves a thorough investigation for future research. We also recognize that other pathways to adverse outcomes exist in CHD neonates, including genetic etiologies. Understanding the genetic contributions to WMI risk is an important area for future research.

In conclusion, our findings support the hypothesis that WMI in the term neonate with CHD occurs on a substrate of delayed brain maturation and points to the urgent need for preventive strategies of this prevalent brain injury.

ACKNOWLEDGEMENT

REFERENCES

Adams E, Chau V, Poskitt KJ, Grunau RE, Synnes A, Miller SP (2010). "Tractography-based quantitation of corticospinal tract development in premature newborns." J Pediatr 156:882–888, 888.e881. [PubMed: 20227731]

Andropoulos DB, Hunter JV, Nelson DP, Stayer SA, Stark AR, McKenzie ED, Heinle JS, Graves DE and Fraser CD (2010). "Brain immaturity is associated with brain injury before and after neonatal cardiac surgery with high-flow bypass and cerebral oxygenation monitoring."" The Journal of thoracic and cardiovascular surgery 139: 543–556. [PubMed: 19909994]

Avants BB, Epstein CL, Grossman M and Gee JC (2008). "Symmetric diffeomorphic image registration with cross-correlation: evaluating automated labeling of elderly and neurodegenerative brain." Med Image Anal 12(1): 26–41. [PubMed: 17659998]

Back SA (2014). "Cerebral white and gray matter injury in newborns: new insights into pathophysiology and management." Clinics in perinatology 41: 1–24. [PubMed: 24524444]

Back SA and Miller SP (2014). "Brain injury in premature neonates: A primary cerebral dysmaturation disorder?" Ann Neurol 75(4): 469–486. [PubMed: 24615937]

Bassi L, Chew A, Merchant N, Ball G, Ramenghi L, Allsop JM, Doria V, Arichi T, Mosca F, Edwards AD, Cowan FM, Rutherford MA, and Counsell SJ (2011). "Diffusion tensor imaging in preterm infants with punctate white matter lesions." Pediatr Res 69:561–566. [PubMed: 21386750]

Beca J, Gunn JK, Coleman L, Hope A, Reed PW, Hunt RW, Finucane K, Brizard C, Dance B and Shekerdemian LS (2013). "New white matter brain injury after infant heart surgery is associated with diagnostic group and the use of circulatory arrest." Circulation 127: 971–979. [PubMed: 23371931]

Block AJ, McQuillen PS, Chau V, Glass H, Poskitt KJ, Barkovich AJ, Esch M, Soulikias W, Azakie A, Campbel A and Miller SP (2010). "Clinically silent preoperative brain injuries do not worsen with surgery in neonates with congenital heart disease." J Thorac Cardiovasc Surg 140(3):550–557. [PubMed: 20434174]

Buser JR, Maire J, Riddle A, Gong X, Nguyen T, Nelson K, Luo NL, Ren J, Struve J, Sherman LS, Miller SP, Chau V, Hendson G, Ballabh P, Grafe MR and Back SA (2012). "Arrested preoligodendrocyte maturation contributes to myelination failure in premature infants." Ann Neurol 71(1): 93–109. [PubMed: 22275256]

Clouchoux C, du Plessis AJ, Bouyssi-Kobar M, Tworetzky W, McElhinney DB, Brown DW, Gholipour A, Kudelski D, Warfield SK, McCarter RJ, Robertson RL, Evans AC, Newburger JW and Limperopoulos C (2013). "Delayed cortical development in fetuses with complex congenital heart disease." Cerebral cortex (New York, N.Y.1991) 23: 2932–2943.

Dimitropoulos A, McQuillen PS, Sethi V, Moosa A, Chau V, Xu D, Brant R, Azakie A, Campbell A, Barkovich AJ, Poskitt KJ and Miller SP (2013). "Brain injury and development in newborns with critical congenital heart disease." Neurology 81(3): 241–248. [PubMed: 23771484]

Fietz SA, Kelava I, Vogt J, Wilsch-Brauninger M, Stenzel D, Fish JL, Corbeil D, Riehn A, Distler W, Nitsch R, Huttner WB (2010). "OSVZ progenitors of human and ferret neocortex are epithelial-like and expand by integrin signaling." Nat Neurosci 13:690–699. [PubMed: 20436478]

Friedel M, van Eede MC, Pipitone J, Chakravarty MM and Lerch JP (2014). "Pydpiper: a flexible toolkit for constructing novel registration pipelines." Frontiers in neuroinformatics 8: 67. [PubMed: 25126069]

Goff DA, Luan X, Gerdes M, Bernbaum J, D'Agostino JA, Rychik J, Wernovsky G, Licht DJ, Nicolson SC, Clancy RR, Spray TL and Gaynor JW (2012). "Younger gestational age is associated with worse neurodevelopmental outcomes after cardiac surgery in infancy." The Journal of thoracic and cardiovascular surgery 143: 535–542. [PubMed: 22340027]

Guo T, Duerden EG, Adams E, Chau V, Branson HM, Chakravarty MM, Poskitt KJ, Synnes A, Grunau RE and Miller SP (2017). "Quantitative assessment of white matter injury in preterm neonates: Association with outcomes." Neurology 88(7): 614–622. [PubMed: 28100727]

He L, Parikh NA (2015). "Aberrant Executive and Frontoparietal Functional Connectivity in Very Preterm Infants With Diffuse White Matter Abnormalities." Pediatr Neurol 53:330–337. [PubMed: 26216502]

Karmacharya S, Gagoski B, Ning L, Vyas R, Cheng HH, Soul J, Newberger JW, Shenton ME, Rathi Y, and Grant PE (2018). "Advanced diffusion imaging for assessing normal white matter development in neonates and characterizing aberrant development in congenital heart disease." NeuroImage Clin 19: 360–373. [PubMed: 30013919]

Kostovic I, Judas M, Rados M and Hrabac P (2002). "Laminar organization of the human fetal cerebrum revealed by histochemical markers and magnetic resonance imaging." Cereb Cortex 12(5): 536–544. [PubMed: 11950771]

Li AM, Chau V, Poskitt KJ, Sargent MA, Lupton BA, Hill A, Roland E and Miller SP (2009). "White matter injury in term newborns with neonatal encephalopathy." Pediatric research 65: 85–89. [PubMed: 18787422]

Licht DJ, Shera DM, Clancy RR, Wernovsky G, Montenegro LM, Nicolson SC, Zimmerman RA, Spray TL, Gaynor JW and Vossough A (2009). "Brain maturation is delayed in infants with

complex congenital heart defects." The Journal of thoracic and cardiovascular surgery 137: 529–536; discussion 536–527. [PubMed: 19258059]

Licht DJ, Wang J, Silvestre DW, Nicolson SC, Montenegro LM, Wernovsky G, Tabbutt S, Durning SM, Shera DM, Gaynor JW, Spray TL, Clancy RR, Zimmerman RA and Detre JA (2004). "Preoperative cerebral blood flow is diminished in neonates with severe congenital heart defects." The Journal of thoracic and cardiovascular surgery 128: 841–849. [PubMed: 15573068]

Lim JM, Kingdom T, Saini B, Chau V, Post M, Blaser S, Macgowan C, Miller SP and Seed M (2016). "Cerebral oxygen delivery is reduced in newborns with congenital heart disease." The Journal of thoracic and cardiovascular surgery 152: 1095–1103. [PubMed: 27349283]

Limperopoulos C, Tworetzky W, McElhinney DB, Newburger JW, Brown DW, Robertson J, Richard L, Guizard N, McGrath E, Geva J, Annese D, Dunbar-Masterson C, Trainor B, Laussen PC and du Plessis AJ (2010). "Brain volume and metabolism in fetuses with congenital heart disease: evaluation with quantitative magnetic resonance imaging and spectroscopy." Circulation 121(1): 26–33. [PubMed: 20026783]

Mahle WT, Tavani F, Zimmerman RA, Nicolson SC, Galli KK, Gaynor JW, Clancy RR, Montenegro LM, Spray TL, Chiavacci RM, Wernovsky G and Kurth CD (2002). "An MRI study of neurological injury before and after congenital heart surgery." Circulation 106: I109–I114. [PubMed: 12354718]

Marelli A, Miller SP, Marino BS, Jefferson AL and Newburger JW (2016). "Brain in Congenital Heart Disease Across the Lifespan: The Cumulative Burden of Injury." Circulation 133: 1951–1962. [PubMed: 27185022]

Martinez-Biarge M, Jowett VC, Cowan FM and Wusthoff CJ (2013). "Neurodevelopmental outcome in children with congenital heart disease." Seminars in fetal \ & neonatal medicine 18: 279–285. [PubMed: 23706956]

Martinez-Cerdeno V, Cunningham CL, Camacho J, Antczak J, Prakash AN, Cziep ME, Walker AI, and Noctor SC (2012). "Comparative analysis of the subventricular zone in rat, ferret and macaque: evidence for an outer subventricular zone in rodents." PLoS One 7:e30178. [PubMed: 22272298]

McQuillen PS, Barkovich AJ, Hamrick SEG, Perez M, Ward P, Glidden DV, Azakie A, Karl T and Miller SP (2007). "Temporal and anatomic risk profile of brain injury with neonatal repair of congenital heart defects." Stroke 38: 736–741. [PubMed: 17261728]

McQuillen PS and Miller SP (2010). "Congenital heart disease and brain development." Annals of the New York Academy of Sciences 1184: 68–86. [PubMed: 20146691]

Miller SP, McQuillen PS, Hamrick S, Xu D, Glidden DV, Charlton N, Karl T, Azakie A, Ferriero DM, Barkovich AJ and Vigneron DB (2007). "Abnormal brain development in newborns with congenital heart disease." N Engl J Med 357(19): 1928–1938. [PubMed: 17989385]

Miller SP, McQuillen PS, Vigneron DB, Glidden DV, Barkovich AJ, Ferriero DM, Hamrick SEG, Azakie A and Karl TR (2004). "Preoperative brain injury in newborns with transposition of the great arteries." The Annals of thoracic surgery 77: 1698–1706. [PubMed: 15111170]

Morton PD, Ishibashi N and Jonas RA (2017). "Neurodevelopmental Abnormalities and Congenital Heart Disease: Insights Into Altered Brain Maturation." Circulation research 120: 960–977. [PubMed: 28302742]

Mulkey SB, Ou X, Ramakrishnaiah RH, Glasier CM, Swearingen CJ, Melguizo MS, Yap VL, Schmitz ML, and Bhutta AT (2014). "White matter injury in newborns with congenital heart disease: a diffusion tensor imaging study." Pediatr Neurol 51(3): 377–383. [PubMed: 25160542]

Partridge SC, Vigneron DB, Charlton NN, Berman JI, Henry RG, Mukherjee P, McQuillen PS, Karl TR, Barkovich AJ and Miller SP (2006). "Pyramidal tract maturation after brain injury in newborns with heart disease." Annals of neurology 59: 640–651. [PubMed: 16450369]

Petit CJ, Rome JJ, Wernovsky G, Mason SE, Shera DM, Nicolson SC, Montenegro LM, Tabbutt S, Zimmerman RA and Licht DJ (2009). "Preoperative brain injury in transposition of the great arteries is associated with oxygenation and time to surgery, not balloon atrial septostomy." Circulation 119: 709–716. [PubMed: 19171858]

Peyvandi S, De Santiago V, Chakkarapani E, Chau V, Campbell A, Poskitt KJ, Xu D, Barkovich AJ, Miller S and McQuillen P (2016). "Association of Prenatal Diagnosis of Critical Congenital Heart

Disease With Postnatal Brain Development and the Risk of Brain Injury." JAMA pediatrics 170: e154450. [PubMed: 26902528]

Raybaud C, Ahmad T, Rastegar N, Shroff M and Al Nassar M (2013). "The premature brain: developmental and lesional anatomy." Neuroradiology 55 Suppl 2: 23–40. [PubMed: 23832006]

Riddle A, Luo NL, Manese M, Beardsley DJ, Green L, Rorvik DA, Kelly KA, Barlow CH, Kelly JJ, Hohimer AR and Back SA (2006). "Spatial heterogeneity in oligodendrocyte lineage maturation and not cerebral blood flow predicts fetal ovine periventricular white matter injury." The Journal of neuroscience : the official journal of the Society for Neuroscience 26: 3045–3055. [PubMed: 16540583]

Rudolph AM (2016). "Impaired cerebral development in fetuses with congenital cardiovascular malformations: Is it the result of inadequate glucose supply?" Pediatric research 80: 172–177. [PubMed: 27055190]

Steurer MA, Baer RJ, Keller RL, Oltman S, Chambers CD, Norton ME, Peyvandi S, Rand L, Rajagopal S, Ryckman KK, Moon-Grady AJ and Jelliffe-Pawlowski LL (2017). "Gestational Age and Outcomes in Critical Congenital Heart Disease." Pediatrics 140.

Sun L, Macgowan CK, Sled JG, Yoo S-J, Manlhiot C, Porayette P, Grosse Wortmann L, Jaeggi E, McCrindle BW, Kingdom J, Hickey E, Miller S and Seed M (2015). "Reduced fetal cerebral oxygen consumption is associated with smaller brain size in fetuses with congenital heart disease." Circulation 131: 1313–1323. [PubMed: 25762062]

Smyser CD, Snyder AZ, Shimony JS, Blazey TM, Inder TE, Neil JJ (2013). "Effects of white matter injury on resting state fMRI measures in prematurely born infants." PLoS One 8:e68098. [PubMed: 23874510]

Tusor N, Benders MJ, Counsell SJ, Nongena P, Ederies MA, Falconer S, Chew A, Gonzalez-Cinca N, Hajnal JV, Gangadharan S, Chatzi V, Kersbergen KJ, Kennea N, Azzopardi DV, and Edwards AD (2017). "Punctate white matter lesions associated with altered brain development and adverse motor outcome in preterm infants." Sci Rep 7(1): 13250. [PubMed: 29038505]

Volpe JJ (2000). "Overview: normal and abnormal human brain development." Mental retardation and developmental disabilities research reviews 6: 1–5. [PubMed: 10899791]

von Rhein M, Buchmann A, Hagmann C, Dave H, Bernet V, Scheer I, Knirsch W, Latal B, Heart and B. R. Group (2015). "Severe Congenital Heart Defects Are Associated with Global Reduction of Neonatal Brain Volumes." The Journal of pediatrics 167: 1259–1263.e1251. [PubMed: 26233604]

von Rhein M, Buchmann A, Hagmann C, Huber R, Klaver P, Knirsch W and Latal B (2014). "Brain volumes predict neurodevelopment in adolescents after surgery for congenital heart disease." Brain a journal of neurology 137: 268–276. [PubMed: 24277720]

Peyvandi S, Chau V, Guo T, Xu D, Glass HC, Synnes A, Poskitt K, Barkovich AJ, Miller SP, McQuillen PS. (2018). "Neonatal brain injury and timing of neurodevelopmental assessment in patients with congenital heart disease." J Am Coll Cardiol 71(18): 1986–1996. [PubMed: 29724352]

Figure 1. Total WMI Volumes in UBC, UCSF, and UCZ Term CHD Neonates and UBC Preterm Neonates at Early MRI and Term MRI (mm^3)

The total WMI volumes of 29 UBC, 43 UCSF, and 14 UCZ term neonates with CHD, and those of UBC preterm newborns at early-in-life (58 images, median postmenstrual age [PMA]: 32.2 weeks) and TEA (41 images, median PMA: 41 weeks). UBC-CHD (median=84.6mm^3, IQR=26–174.7mm^3); UCSF-CHD (median=104mm^3, IQR=44–243mm^3); UCZ-CHD (median=121mm^3, IQR=68–200.8mm^3); UBC-Prem at early-in-life (median: 43.4mm^3, IQR=19.5–361.3mm^3); UBC-Prem at TEA (median: 175.8mm^3, IQR=73.8– 306.0mm^3).
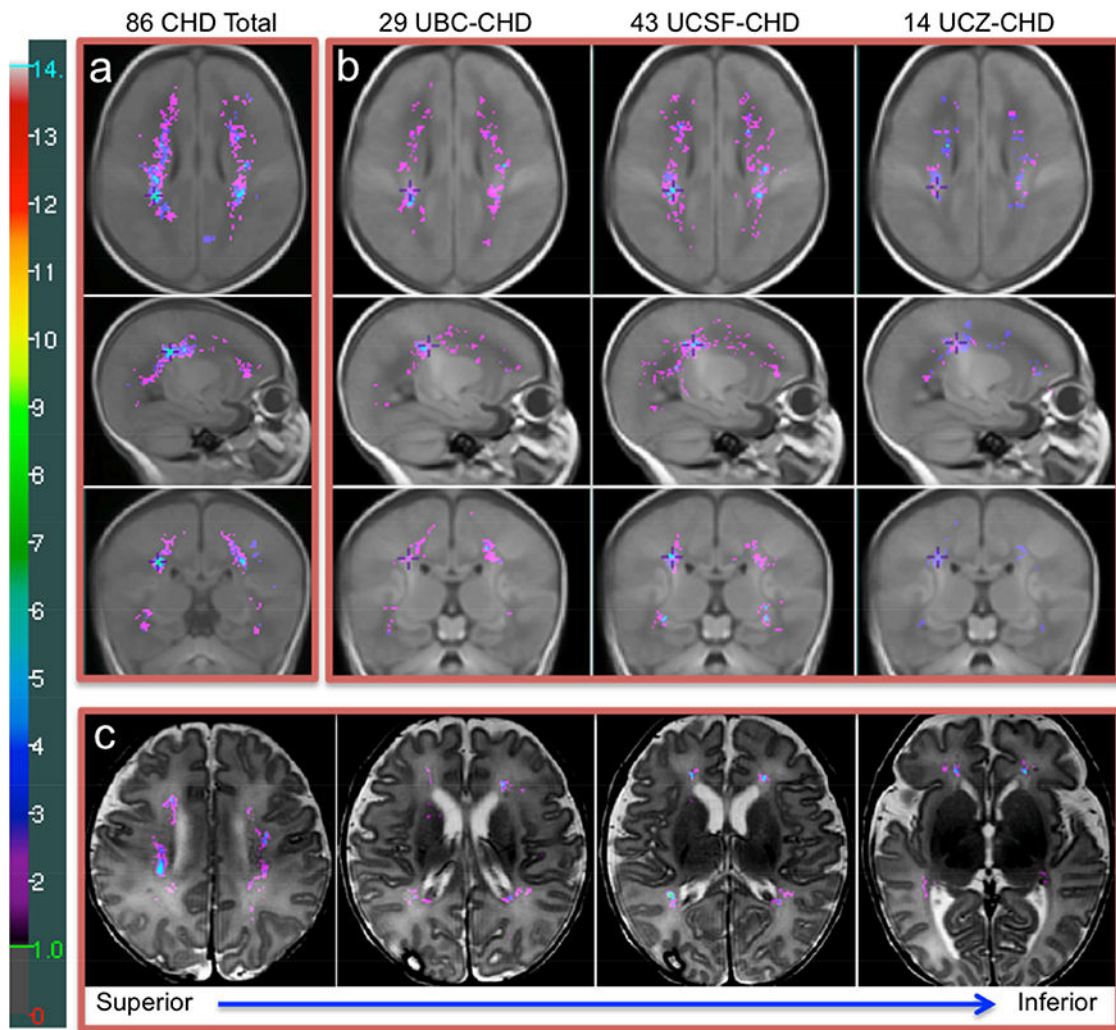
Figure 2. The Probabilistic WMI Map of 86 CHD Neonates and WMI Maps of Three Centres
(a) The probabilistic WMI map of 86 term neonates with CHD overlaid on the T1-weighted term brain template, (b) the WMI maps of 29 UBC, 43 UCSF, and 14 UCZ CHD neonates respectively, (c) the WMI map of 86 CHD neonates overlaid on a T2-weighted image (punctate WMI that occurred in two or more term CHD neonates at a homologous region are shown in this colour map and WMI seen only in a single neonate are omitted). **a:** The cumulative (summed) WMI map of 86 neonates is overlaid on the term brain template (median age: 40.3 weeks, IQR=39.7–40.7) in axial (top), sagittal (middle), and coronal (bottom) planes. The colour bar on the left indicates the colour coding of the WMI summation. The maximum value on the map is 10. The cross on the three planes of the brain template in the same column of the WMI map is placed at the exactly identical location. **b:** The cumulative WMI maps of 29 UBC, 43 UCSF, and 14 UCZ term CHD neonates overlaid on the same term brain template respectively. **c:** The probabilistic WMI map of 86 term CHD neonates nonlinearly transformed and overlaid on the high-resolution T2-weighted image of a CHD neonate (postmenstrual age [PMA]: 40.7 weeks). The lesions are seen in subventricular zone and intermediate zone. The axial planes along the superior to inferior direction are displayed from left to right in the figure.
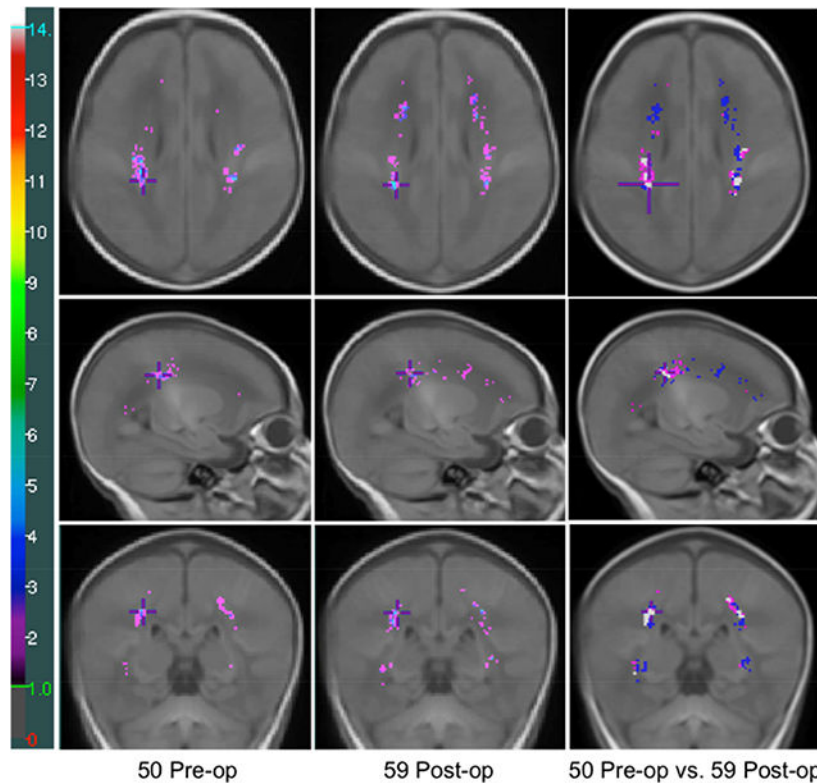
Figure 3. Comparison of Pre- and Post-operatively Identified WMI in CHD Neonates
The probabilistic WMI maps of 50 pre-operative (1st column, median age: 40 weeks, IQR: 38.6–41.2) and 59 post-operative (2nd column, median age: 41.9 weeks, IQR: 40.5–43.2) images of CHD neonates, and the comparison of the pre- and post-operatively identified WMI (3rd column). The colour bar on the left indicates the colour coding of the WMI summation. The maximum values on the pre- and post-operative maps are 6 and 9 respectively. 3rd column: Voxels in magenta: WMI identified only on pre-op images; Voxels in blue: WMI identified only on post-op images; Voxels in white: WMI identified in both pre- and post-operative images. Punctate WMI that occurred in two or more term CHD neonates at a homologous region are shown in the colour maps and WMI seen only in a single neonate are omitted.

Figure 4. Comparison of WMI Distribution between Term CHD Neonates and Preterm Neonates
a) Comparison of the WMI map of 86 term CHD neonates and that of 58 preterm newborns scanned early-in-life overlaid on the T1-weighted term brain template, (b) Comparison of the WMI map of 86 term CHD neonates and that of 41 preterm newborns scanned at TEA overlaid on the T1-weighted term brain template. Punctate WMI that occurred in two or more term CHD neonates at a homologous region are shown in the co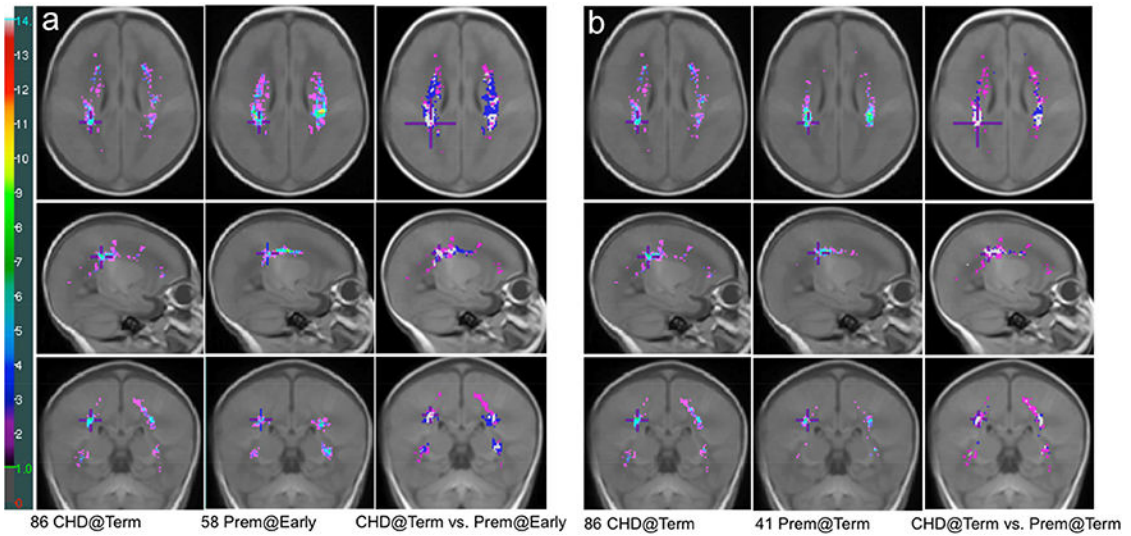lour maps and WMI seen only in a single neonate are omitted. **a**-1st column: The cumulative (summed) WMI map of 86 term CHD neonates is overlaid on the term brain template in axial (top), sagittal (middle), and coronal (bottom) planes; **a**-2nd column: The cumulative WMI map of 58 preterm newborns scanned early-in-life; **a**-3rd column: Comparison of term CHD WMI and preterm WMI at early-in-life. **b**-1st column: The cumulative (summed) WMI map of 86 term CHD neonates is overlaid on the term brain template in axial (top), sagittal (middle), and coronal (bottom) planes; **b**-2nd column: The cumulative WMI map of 41 preterm newborns scanned at TEA; **b**-3rd column: Comparison of term CHD WMI and preterm WMI at TEA. In a-3rd and b-3rd columns, Magenta: WMI identified only in CHD neonates; Blue: WMI identified only in preterm neonates; White: WMI common to both CHD and preterm neonates. The colour bar on the left indicates the colour coding of the WMI summation. The maximum values on the term CHD, preterm at early-in-life, and preterm at TEA maps are 10, 14, and 12 respectively. The cross on the three planes of the brain template in the same column of the WMI map is placed at the exactly identical location.

Table 1.

Clinical Factors and Demographics for Term CHD Neonates in UBC, UCSF, UCZ

	UBC n=76	UCSF n=125	UCZ n=15	p
Males, No. (%)	**54 (71.1%)**	**79 (63.2%)**	**11 (73.3%)**	**0.442**
Heart lesion type (%) 1. Transposition of the great arteries	52 (68.4%)	55 (45.8%)	11 (73.3%)	
2. Single ventricle physiology	14 (18.4%)	48 (40%)	2 (13.3%)	**0.008***
3. Others	10 (13.2%)	17 (14.2%)	2 (13.3%)	
Birth gestational age, weeks Median [IQR]	39 [38–40]	39 [38–40]	39.2 [38.8–40.1]	0.446
Birth weight, kg Median [IQR]	3.23 [2.94–3.76]	3.25 [2.98–3.58]	3 [2.79–3.46]	0.607
Birth head circumference cm Median [IQR]	34 [33–35]	34 [33–35.4]	34 [33.5–35.5]	0.851
Inborn (%)	45 (59.2%)	49 (39.5%)	6 (40%)	**0.022***
Small for gestational age (%)	3 (3.9%)	8 (7.0%)	3 (20%)	0.079
Prenatal diagnosis (%)	41 (53.9%)	55 (44.4%)	2 (13.3%)	**0.014***
Apgar score at 5 minutes Median [IQR]	10 [9–10]	10 [9–10]	9 [8–9]	**0.002***
SNAP-PE Median [IQR]	19 [7.5–27.5]	15 [11–19.3]	NA	**0.226**
Lowest saturation level pre-operative (Arterial) Median [IQR]	72 [54–83]	71.5 [57.8–82]	57.5 [32–68.3]	**0.008***
Balloon atrial septostomy (%)	42 (55.3%)	34 (28.3%)	9 (60%)	**<0.001***
Cardiopulmonary bypass time, minutes Median [IQR]	157 [132–206]	124 [101.3–146]	187 [170.3–207.5]	**<0.001***
Deep hypothermic circulatory arrest, minutes Median [IQR]	0 [0–5.5]	0 [0–6]	0 [0–0]	**0.009**
Lowest mean blood pressure post-operative day 1, mmHg Median [IQR]	40 [36.3–43]	NA	38 [35–39]	**0.028***
Age at MRI, weeks Median [IQR]	40.3 [39.3–41.6]	40.4 [39.4–41.7]	40.6[39.8–42.6]	0.591
Stroke (%)	17 (23.3%)	25 (23.4%)	3 (33.3%)	0.79

Table 2a.

Association of Birth Gestational Age with Maximum Total WMI volume and WMI percentage in Term CHD Neonates

	WMI volume			Percent of WMI to Total Cerebral Volume		
	Coef.	95% CI	p	Coef.	95% CI	p
Birth gestational age (GA)	−20.06	−34.46 - −5.67	**0.006***	−0.008	−0.013 - −0.003	**0.003***
Centre_1	−36.29	−116.19 – 43.62	0.373	−0.006	−0.034 – 0.022	0.69
Centre_2	− 2.92	−85.12 – 79.28	0.944	0.010	−0.02 – 0.039	0.518
Centre_3	Reference			Reference		
TGA	−77.96	−156.05 – 0.14	0.05	−0.031	−0.06 - −0.002	**0.034***
SVP	−62.37	−141.12 – 16.39	0.121	−0.028	−0.057 – 0.001	0.055
Other	Reference			Reference		
Lowest arterial saturation level pre-operative	−1.24	−2.42 - −0.07	**0.038***	−0.001	−0.001 – 0	**0.008***
Total bypass time	0.38	0.03 – 0.74	**0.035***	0.0001	1.12E-5 – 0.0001	**0.03***
Lowest mean blood pressure post-operative	−1.13	−4.21 – 1.95	0.471	0.0001	−0.002 – 0.001	0.378

Table 2b.

Association of Birth Gestational Age with Pre-operative Total WMI volume and WMI percentage in Term CHD Neonates

	Pre-op WMI volume			*Percent of Pre-op WMI to Total Cerebral Volume*		
	Coef.	*95% CI*	*p*	*Coef.*	*95% CI*	*p*
Birth gestational age (GA)	−42.19	−75.23 - −9.15	**0.012***	−0.015	−0.027 - −0.003	**0.011***
Centre_1	−395.71	−577.96 - −213.46	**<0.001***	−0.131	−0.195 - −0.068	**<0.001***
Centre_2	−405.12	−583.19 - −227.06	**<0.001***	−0.133	−0.195 - −0.07	**<0.001***
Centre_3	Reference			Reference		
TGA	45.66	−106.83 – 198.14	0.557	0.017	−0.039 – 0.072	0.558
SVP	4.51	−146.95 – 155.97	0.953	0.001	−0.053 – 0.056	0.965
Other	Reference			Reference		
Lowest arterial saturation level pre-operative	0.512	−2.13 – 3.15	0.704	0.000	−0.001 – 0.001	0.83